Light trapping in conformal CuO/Si pyramids heterojunction for self-powered broadband photodetection

Jing-Yue Li, Long-Qiang Shan, Li-Yan Liang, Shi-Rong Chen, Li Wang, Yu-Xue Zhou，
Chun-Yan Wu, Lin-Bao Luo, Senior Member, IEEE

***Abstract*—In this letter, we report a conformal CuO/Si micropyramids heterojunction photodetector fabricated by RF reactive magnetron sputtering CuO nanofilm onto the dense and random Si micropyramids. The device presents a prominent photovoltaic effect over the broad wavelength range (300-1300 nm), which enables efficient self-powered broadband photodetection, giving a peak responsivity of 279 mA/W and specific detectivity of 1.18 × 10^{11} Jones at zero bias upon 810 nm illumination at light intensity of 5.9 μW/cm^2. Compared to its planar Si counterpart, the conformal CuO/Si pyramids heterojunction photodetector shows a significantly enhanced photoresponse over the broadband region. According to the theoretical simulation of photon absorption in Si pyramid structures, this should be ascribed to the pronounced light trapping effect of the pyramid structures. The light-matter interaction in the heterojunction was accordingly enhanced, leading to the improved photoresponse. This work is well compatible with the current complementary metal-oxide semiconductor (CMOS) technology and provides a facile and effective strategy for the on-chip high performance photodetection.**

***Index Terms*—Si pyramids, self-powered photodetector, light trapping**

I. Introduction

Silicon (Si) is the second abundant element in the earth, which has attracted great attention in the field of electronic and optoelectronic devices owing to its high carrier mobility, long-term stability and the well-established Si-based semiconductor manufacturing techniques. Thanks to its suitable bandgap (~1.12 eV), Si-based photodetectors have become the most commonly used commercial photodetectors for visible light detection (450-800 nm) [1]. However, the performance of planar Si-based photodetectors is limited by the high optical reflection loss of polished crystalline Si in the visible region (up to 40%) [2]. Extensive efforts have been devoted to improving the efficiency of light harvesting and subsequently the performance of Si-based photodetectors. For example, light trapping effect of Si micro/nanostructures [3-6], including Si microholes, Si nanowires and Si micropyramids (both upright and inverted), has been well demonstrated in both experiment and simulation.

Si pyramids, especially the random pyramids, stand out from the textured Si due to their intriguing merits: (1) Random micro/nanostructures are more helpful to achieve broadband enhancement of light absorption. Light reflection of upright Si pyramids can be suppressed to about 10% within the broadband wavelength region (400-1000 nm) [7] and near-Lambertian light trapping effect can be achieved in ultrathin crystalline Si (30 μm) by utilizing random Si micropyramids [8]. (2) The surface area of Si pyramids is only 1.7-fold their planar Si counterpart, remarkably lower than that of other Si nanostructures [9].This gives rise to a lower surface recombination and facilitates the higher efficiency of light harvesting. (3) Random upright pyramids can be easily constructed on the upper surface of Si through the anisotropic wet etching in alkaline solution [10]. Neither complicated photolithography process nor precisely controlled mask is required, making it practical for larger-scale and low-cost manufacturing.

Herein, the conformal CuO/Si micropyramids heterojunction was fabricated, which functioned well as a self-powered photodetector over a broad wavelength region (300-1300 nm). The remarkably enhanced photoresponse compared to its planar Si counterpart has also been revealed by the theoretical simulation based on Silvaco Technology Computer Aided Design (TCAD).

II. Experiments

A. Device Fabrication

For the fabrication of the self-powered CuO/Si pyramids heterojunction photodetector, CuO film was deposited onto Si pyramids through RF reactive magnetron sputtering for 30 min to form a conformal heterojucntion, using a high-purity Cu

This work was supported in part by the National Natural Science Foundation of China under Grant 62074048, in part by the Natural Science Foundation of Anhui Province under Grant 2108085MF229 and Grant 2208085MF177, in part by the Key Research and Development Plan of Anhui Province under Grant 2022f04020007 and in part by the Fundamental Research Funds for the Central Universities under Grant PA2020GDKC0014 and Grant JZ2018HGXC0001. (*Corresponding authors: Shi-Rong Chen; Yu-Xue Zhou; Chun-Yan Wu.*)

Jing-Yue Li, Long-Qiang Shan, Li-Yan Liang, Shi-Rong Chen, Li Wang, Chun-Yan Wu, Lin-Bao Luo are with the School of Microelectronics, Hefei University of Technology, Hefei 230009, China. (E-mail: srchen@hfut.edu.cn; cywu@hfut.edu.cn)

Yu-Xue Zhou is with College of Physical Science and Technology, Yangzhou University, Yangzhou 225002, China. (E-mail: yxzhou@yzu.edu.cn)

This article has been accepted for publication in IEEE Photonics Technology Letters. This is the author's version which has not been fully edited and content may change prior to final publication. Citation information: DOI 10.1109/LPT.2022.3205028

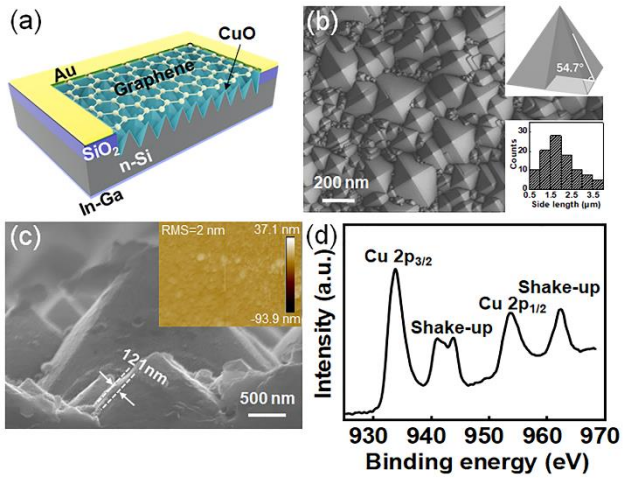

Fig. 1. (a) Schematic illustration of the CuO/Si pyramids heterojunction photodetector. (b) The bird-view SEM image of Si pyramid arrays. The inset shows the side length distribution of Si pyramids. (c) A typical cross-sectional SEM image of CuO/Si pyramids hybrid structure, the inset shows AFM image of CuO film. (d) Cu 2p core level XPS spectrum.

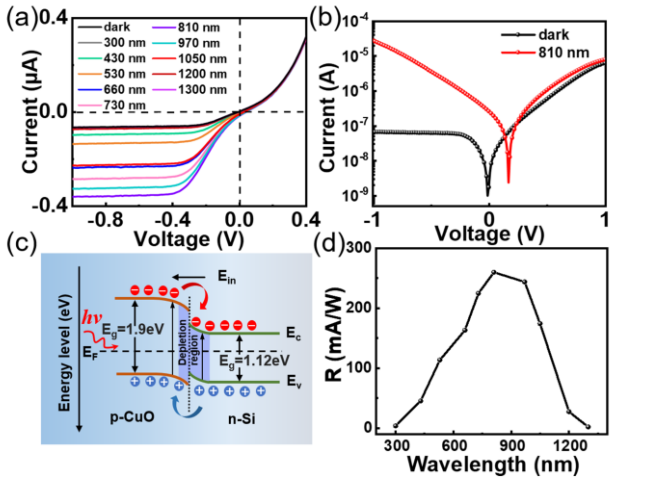

Fig. 2. (a) *I-V* curves of the device in the dark and upon illumination with different wavelengths (light intensity: 10.3 μW/cm^2). (b) *I-V* curves of the device in the dark and upon 810 nm illumination in a semilogarithmic scale. (c) The energy band diagram of the CuO/Si heterojunction upon illumination at zero bias. (d) Spectral response of the device at zero bias (light intensity: 10.3 μW/cm^2).

target and the mixed gas of Ar (20 sccm) and O_2 (15 sccm) as the working gas [11]. In a typical process for the fabrication of Si random micropyramids, a 2 × 2 mm^2 window was firstly defined on a pre-cleaned *n*-type lightly doped (100) Si wafer (doping concentration: ~10^{15} cm^{-3}) with 300 nm SiO_2 insulating layer through photolithography method, followed by etching in a buffered oxide etch solution (BOE, HF: NH_4F: H_2O=3 mL: 6 g: 10 mL) to remove the unprotected SiO_2 layer within the window. Dense and random Si micropyramids were then formed *via* anisotropic etching in a mixture solution of NaOH: $(CH_3)_2CHOH$: H_2O (3 g: 3 ml: 54 ml) at 80ºC for 40 min. In-Ga alloy was pasted onto the rear side of the Si wafer to function as the bottom electrode and a layer of chemical vapor deposition (CVD)-grown monolayer graphene was adopted as the top electrode, which was transferred to the top of heterojunction through the polymethylethacrylate (PMMA)-assisted wet transfer method and facilitated the high-efficient collection of photo-generated carriers.

B. Device Characterization and Theoretical Simulation

Photoelectronic characterization of the CuO/Si pyramids heterojunction was conducted on a semiconductor characterization system (Keithley 4200-SCS) at room temperature. Laser diodes with different wavelengths (Thorlabs, 300-1300 nm) were used as light sources, whose intensities were carefully calibrated before measurement by using a power meter (Thorlabs GmbH., PM 100D).

The photon absorption of Si pyramid arrays and its planar Si counterpart was simulated by using the 2D optoelectronic simulator Luminous of Silvaco TCAD. Average side length l=2 μm and height h=1.4 μm of the Si pyramids were used as the structural parameters for modeling, which were extracted from scanning electron microscope (SEM) images of the experimental sample. For the periodic micropyrimads along the horizontal direction, the finite difference time domain (FDTD) method was chosen to describe the wave propagation of light incident from the top at a 90° incident angle [12]. Perfectly matched layer (PML) boundary conditions were applied on the vertical direction.

III. Results and Discussion

Fig. 1(a) illustrates the schematic of CuO/Si pyramids heterojunction photodetector and the morphologies of the as-etched Si pyramid arrays as well as the CuO/Si pyramids hybrid structure were characterized by SEM images presented in Fig. 1(b) and (c). As we know that the formation of Si pyramids should be ascribed to the anisotropic wet etching of (100) and (111) planes of Si wafer in the alkaline solution, which leads to a 54.7° slope of the sidewall surface (inset in Fig. 1(b)) [13]. Statistical distribution reveals that the side length of as-obtained Si pyramids ranges from 0.5 to 4.0 μm, giving an average value of about 2.0 μm (inset in Fig. 1(b)). Therefore, the average height of Si pyramids can be calculated to be about 1.4 μm. Fig. 1(c) presents the cross-sectional SEM image of the CuO/Si pyramids hybrid structure. Clearly, the sputtered nanofilm tightly wraps around the surface of the Si pyramids, which thickness is measured to be about 121 nm. Atomic force microscope (AFM) image further reveals that the obtained nanofilm was continuous and uniform, showing a relatively smooth surface with the root mean square roughness of about 2 nm. The composition of the obtained nanofilm was characterized by X-ray photoelectron spectroscopy (XPS) and the Cu 2p core level spectrum was presented in Fig. 1(d). The two main peaks located at 933.8 eV and 953.7 eV can be readily indexed to $Cu2p_{3/2}$ and $Cu2p_{1/2}$, respectively. Meanwhile, two high-intensity satellite peaks located at a higher binding energy than the main $Cu2p_{3/2}$ and $Cu2p_{1/2}$ peaks by about 9 eV can be observed, which are the typical characteristics of CuO phase [14]. Hall effect measurement proved the *p*-type conduction, showing the carrier concentration and Hall mobility of 1.96 × 10^{11} cm^{-3} and 2.25 cm^2 V^{-1} s^{-1}, respectively.

Fig. 2(a) plots the current-voltage (*I-V*) curve of the CuO/Si pyramids heterojunction photodetector in the dark and upon illumination with different wavelengths at a fixed light intensity (P_{in}=10.3 μW/cm^2). The device shows a pronounced rectifying behavior in the dark with a rectification ratio of ~10^2 at ±1 V. The lower rectification ratio may arise from the large

This article has been accepted for publication in IEEE Photonics Technology Letters. This is the author's version which has not been fully edited and content may change prior to final publication. Citation information: DOI 10.1109/LPT.2022.3205028

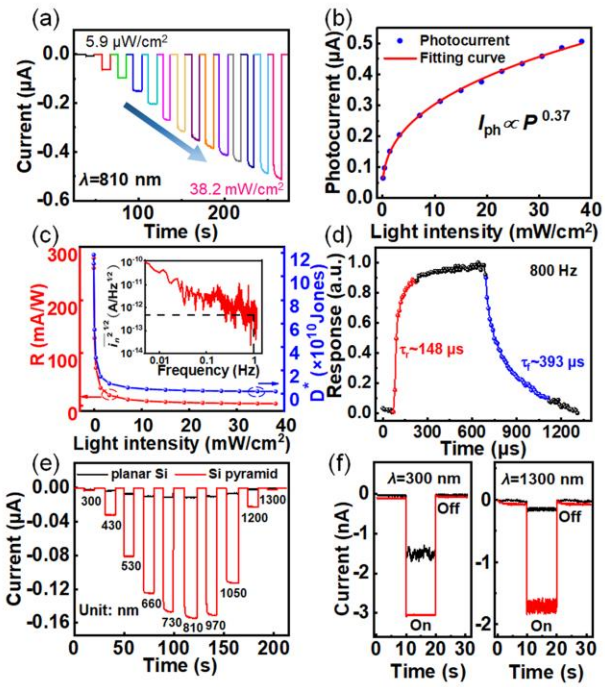

Fig. 3. (a) Time response of the device at zero bias upon 810 nm light illumination with varied light intensities. (b) Photocurrent as a function of light intensity. (c) Responsivity and specific detectivity as a function of light intensity at zero bias. The inset shows the noise spectral density based on the fast Fourier transform of the dark current. (d) A single magnified photoresponse curve at the frequency of 800 Hz to calculate the response time. (e) Time response of the device and its planar Si counterpart at zero bias. (f) Enlarged time response of the device upon 300 and 1300nm illumination.

tunneling current, which could be suppressed by inserting a unipolar barrier [15]. Prominent photoresponse to incident light with broadband wavelengths (300 nm-1300 nm) with a peak photoresponse at 810 nm can also be observed. Significantly, the device exhibits a remarkable photovoltaic characteristics, showing an open-circuit voltage (V_{OC}) of 0.17 V and a short-circuit current (I_{SC}) of 0.26 μA upon 810 nm illumination (Fig. 2(b)). The photovoltaic characteristic could be understood by the energy band diagram shown in Fig. 2(c). Owing to the difference in work function, a built-in electric field with the direction from *n*-Si to *p*-CuO could be formed at the heterojunction interface. Upon illumination, the photo-generated carriers generated within or near the depletion region would be immediately separated toward opposite directions, leading to a photocurrent in the circuit [16]. This photovoltaic behavior of the CuO/Si pyramids heterojunction enables its application as a self-powered photodetector, which can work without external electrical power supply. Responsivity (R) of the device at zero bias was calculated according to the equation $R=(I_{light}-I_{dark})/(S P_{in})$ [17] and plotted in Fig. 2(d), where I_{light} and I_{dark} were the current measured upon light illumination and in the dark, respectively, S was the effective device area (about 0.04 cm^2 for this device). Obviously, the CuO/Si pyramids heterojunction exhibited significant response to incident light over the broad wavelength range.

Time response of the device at zero bias upon 810 nm illumination with varied light intensities was further explored. We can observe from Fig. 3(a) that the device can be steadily

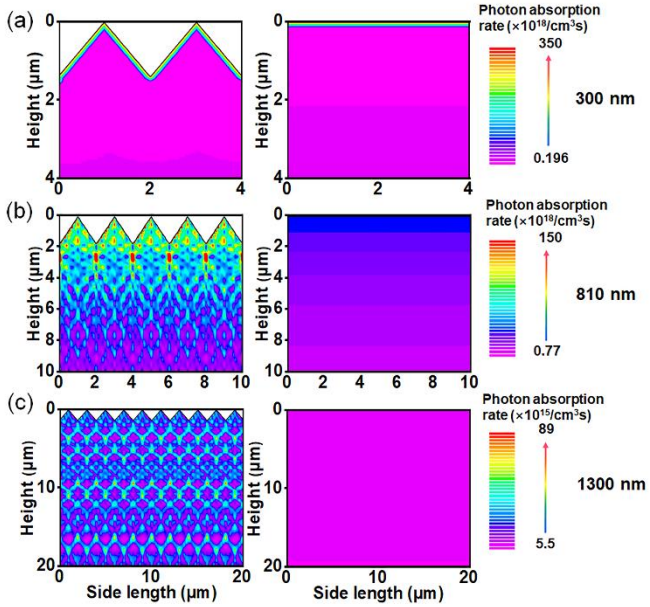

Fig. 4. (a-c) Simulation of photo absorption rate of the Si pyramid arrays and planar Si upon 300, 810 and 1300 nm illumination, respectively.

and fast switched between the "on" and "off" state and the photocurrent monotonously increased from 70 nA to 0.51 μA with the increase of light intensity from 5.9 μW/cm^2 to 38.2 mW/cm^2. The photocurrent as a function of light density was fitted by the power law $I_{ph} \propto P^{\theta}$, giving the exponent θ of 0.37 (Fig. 3(b)). The non-integer exponent θ suggests the existence of recombination loss in the device, which may be inhibited by depositing an ultrathin Al_2O_3 layer for passivation [18]. Furthermore, the other key parameter of the photodetector, specific detectivity (D^*), was calculated using equations of noise equivalent power (NEP): $NEP= \overline{i_n^2}^{1/2} /R$ and $D^*=(S\Delta f)^{1/2}/NEP$ [19], and plotted in Fig. 3(c), where $\overline{i_n^2}^{1/2}$ was the root-mean-square value of the noise current and Δf was the bandwidth. As presented in the inset of Fig. 3(c), the noise spectral density at 1 Hz bandwidth was deduced to be about 4.7×10^{-13} A/Hz$^{1/2}$ from the fast Fourier transform (FFT) of the dark current. R and D^* increased with decreasing light intensity, and reach the highest value of 279 mA/W and 1.18×10^{11} Jones, respectively, at the weak light intensity of 5.9 μW/cm^2. This is reasonable since the recombination loss would be smaller at lower light intensity due to the existence of trap states in the depletion region [20]. Response speed of the device was further measured at the -3 dB bandwidth of the device (about 800 Hz) and plotted in Fig. 3(d), showing the rise/fall time of 148/393 μs, respectively. The performance of the CuO/Si pyramids heterojunction photodetector was comparable to that of the previously reported CuO/Si nanowire [21] and CuO/Si microhole [22] heterojunction photodetectors, revealing the benign heterojunction interface. Notably, the photoresponse of the CuO/Si pyramids heterojunction photodetector was enhanced by at least one order of magnitude than its planar Si counterpart over the wavelength range from 430 nm to 1300 nm (Fig. 3(e) and 3(f)). Even in the UV region (for example, 300 nm), the photocurrent was doubled. We believe that this should be ascribed to the enhanced absorption of the dense and random Si micropyramids arising from the light trapping effect.

Theoretical simulation was further adopted to reveal the light trapping effect of Si pyramids. Fig. 4(a-c) presents the simulated photon absorption rate of the Si pyramids (left) and its planar Si counterpart (right) upon 300, 810 and 1300 nm illumination, respectively. It can be obviously observed that 300 nm incident light was almost absorbed in the very top surface of Si pyramids, showing a highest photon absorption rate in the surface, which decreases with the penetration (Fig. 4(a)). With the increase of wavelengths, the photon absorption rate in the surface decreases and the penetration depth increases accordingly (Fig. 4(b)). This is reasonable since Si possesses a wavelength-dependent absorption coefficient, which declines rapidly with the increase of wavelengths [23]. Notably, despite of the highest photon absorption rate of 300 nm incident light in the surface of Si pyramids, the CuO/Si pyramids heterojunction photodetector presents a pretty low photocurrent upon 300 nm illumination (3.04 nA, shown in Fig. 3(f)). This may be attributed to the higher surface recombination ratio arising from the defects and the interfacial states. For 1300 nm incident light with photon energy lower than the bandgap of Si, the prominent trapping effect of the Si pyramids structure also leads to a remarkably enhanced absorption (Fig. 4(c)). This is believed to arise from the impurities and structural defects in Si [24]. Therefore, the photon absorption of incident light in Si pyramids overpasses that in its planar Si counterpart over the broad wavelength range (300-1300 nm), which enhances the light-matter interaction and results in an improved photoresponse of Si pyramids-based devices [25].

IV. Conclusion

In summary, a conformal CuO/Si pyramids heterojunction photodetector was fabricated through RF reactive magnetron sputtering CuO nanofilm onto the dense and random Si micropyramids. The heterojunction photodetector displayed a prominent photovoltaic effect and functioned well as a self-powered photodetector over the broad wavelength region (300-1300 nm). Comparing to that of its planar Si counterpart, the photoresponse of the CuO/Si pyramids heterojunction photodetector was significantly enhanced, showing a peak responsivity of 279 mA/W and a specific detectivity of 1.18×10^{11} Jones at zero bias upon 810 nm illumination at light intensity of 5.9 μW/cm^2. Theoretical simulation of photon absorption in Si pyramid structures proved that the light-matter interaction in the heterojunction was enhanced by the prominent light trapping effect of the pyramid structures, giving rise to an improved photoresponse. This provides a facile and effective strategy for the high performance Si-based photodetectors.

References

[1] R. Ghalamboland, S. Darbari, M. Rashidifar, and Y. Abdi, "MoS_2/Si-based heterojunction bipolar transistor as a broad band and high sensitivity photodetector," *IEEE Sens. J.*, vol. 21, no. 13, pp. 14784-14788, Jul. 2021, doi: 10.1109/JSEN.2021.3074380.

[2] S. Chhajed, M. F. Schubert, J. K. Kim, and E. F. Schubert, "Nanostructured multilayer graded-index antireflection coating for Si solar cells with broadband and omnidirectional characteristics," *Appl. Phys. Lett.*, vol. 93, no. 25, Dec. 2008, Art. no. 251108, doi: 10.1063/1.3050463.

[3] Y. Sha *et al.*, "High-efficiency SiGe/Si heterojunction phototransistor with photon- trapping nanoholes operating at 600-1000 nm wavelength," *IEEE Trans. Electron Dev.*, vol. 69, no. 5, pp. 2514-2520, May 2022, doi: 10.1109/TED.2022.3162801.

[4] J. Mao *et al.*, "Conformal MoS_2/silicon nanowire array heterojunction with enhanced light trapping and effective interface passivation for ultraweak infrared light detection," *Adv. Funct. Mater.*, vol. 32, no. 11, Mar. 2022, Art. no. 2108174, doi: 10.1002/adfm.202108174.

[5] D. Wu *et al.*, "A defect-induced broadband photodetector based on WS_2/pyramid Si 2D/3D mixed-dimensional heterojunction with a light confinement effect," *Nanoscale*, vol. 13, no. 31, pp. 13550-13557, 2021, doi: 10.1039/D1NR03243G.

[6] H.-J. Syu, H.-C. Chuang, M.-J. Lin, C.-C. Cheng, P.-J. Huang, and C.-F. Lin, "Ultra-broadband photoresponse of localized surface plasmon resonance from Si-based pyramid structures," *Photonics Res.*, vol. 7, no. 10, Oct. 2019, Art. no. 1119, doi: 10.1364/PRJ.7.001119.

[7] H.-Y. Chen *et al.*, "Enhanced photovoltaic performance of inverted pyramid-based nanostructured black-silicon solar cells passivated by an atomic-layer-deposited Al_2O_3 layer," *Nanoscale*, vol. 7, no. 37, pp. 15142-15148, 2015, doi: 10.1039/C5NR03353E.

[8] R. Saive, "Light trapping in thin silicon solar cells: A review on fundamentals and technologies," *Prog. Photovoltaics*, vol. 29, no. 10, pp. 1125-1137, Oct. 2021, doi: 10.1002/pip.3440.

[9] R. P. Srivastava and D. Khang, "Structuring of Si into multiple scales by metal-assisted chemical etching," *Adv. Mater.*, vol. 33, no. 47, Nov. 2021, Art. no. 2005932, doi: 10.1002/adma.202005932.

[10] Q. Chen *et al.*, "Optical properties of a random inverted pyramid textured silicon surface studied by the ray tracing method," *Sol. Energy*, vol. 186, pp. 392-397, Jul. 2019, doi: 10.1016/j.solener.2019.05.031.

[11] J. Li *et al.*, "Effects of oxygen flow rates on the physical characteristics of magnetron sputtered CuO films," *Vacuum*, vol. 168, Oct. 2019, Art. no. 108811, doi: 10.1016/j.vacuum.2019.108811.

[12] *ATLAS User's Manual, Device Simulation Software*, SILVACO Int., Santa Clara, CA, USA, 2018.

[13] J. Wu *et al.*, "The orientation and optical properties of inverted-pyramid-like structures on multi-crystalline silicon textured by Cu-assisted chemical etching," *Sol. Energy*, vol. 171, pp. 675-680, Sep. 2018, doi: 10.1016/j.solener.2018.07.011.

[14] *Handbook of X-ray Photoelectron Spectroscopy*, Perkin-Elmer Corp., Eden Prairie, MN, USA, 1992.

[15] Y. Chen *et al.*, "Unipolar barrier photodetectors based on van der Waals heterostructures," *Nat. Electron.*, vol. 4, no. 5, pp. 357-363, May 2021, doi: 10.1038/s41928-021-00586-w.

[16] Q. Lv, F. Yan, X. Wei, and K. Wang, "High-performance, self-driven photodetector based on Graphene sandwiched GaSe/WS_2 Heterojunction," *Adv. Opt. Mater.*, vol. 6, no. 2, Jan. 2018, Art. no. 1700490, doi: 10.1002/adom.201700490.

[17] J.-M. Liu, *Photonic devices*, Cambridge University Press, Cambridge, UK, 2009.

[18] M. Garin *et al.*, "Black-silicon ultraviolet photodiodes achieve external quantum efficiency above 130%," *Phys. Rev. Lett.*, vol. 125, no. 11, Sep. 2020, Art. no. 117702, doi: 10.1103/PhysRevLett.125.117702.

[19] P. Wu *et al.*, "Van der Waals two-color infrared photodetector," *Light-Sci. Appl.*, vol. 11, no. 1, Dec. 2022, Art. no. 6, doi: 10.1038/s41377-021-00694-4.

[20] K. S. Kim *et al.*, "Ultrasensitive MoS_2 photodetector by serial nano-bridge multi-heterojunction," *Nat Commun.*, vol. 10, no. 1, Dec. 2019, Art. no. 4701, doi: 10.1038/s41467-019-12592-w.

[21] Q. Hong, Y. Cao, J. Xu, H. Lu, J. He, and J.-L. Sun, "Self-powered ultrafast broadband photodetector based on p-n heterojunctions of CuO/Si nanowire array," *ACS Appl. Mater. Interfaces*, vol. 6, no. 23, pp. 20887-20894, Dec. 2014, doi: 10.1021/am5054338.

[22] C. Zhang *et al.*, "Enhanced light trapping in conformal CuO/Si microholes array heterojunction for self-powered broadband photodetection," *IEEE Electron Device Lett.*, vol. 42, no. 6, pp. 883-886, Jun. 2021, doi: 10.1109/LED.2021.3072042.

[23] C.-Y. Tsai, "Interband and intraband absorption coefficients of silicon: Theoretical frameworks and formulations," *IEEE J. Sel. Top. Quantum Electron*, vol. 26, no. 2, pp. 1-10, Mar. 2020, doi: 10.1109/JSTQE.2019.2943389.

[24] S. Huang *et al.*, "Black silicon photodetector with excellent comprehensive properties by rapid thermal annealing and hydrogenated surface passivation," *Adv. Opt. Mater.*, vol. 8, no. 7, Apr. 2020, Art. no. 1901808 doi: 10.1002/adom.201901808.

[25] E. Garnett and P. Yang, "Light trapping in silicon nanowire solar cells," *Nano Lett.*, vol. 10, no. 3, pp. 1082-1087, Mar. 2010, doi: 10.1021/nl100161z.